Ultrasensitive paper based nucleic acid detection realized by three-dimensional DNA-AuNPs network amplification

Ya Gao, Xilei Deng, Wei Wen, Xiuhua Zhang, Shengfu Wang

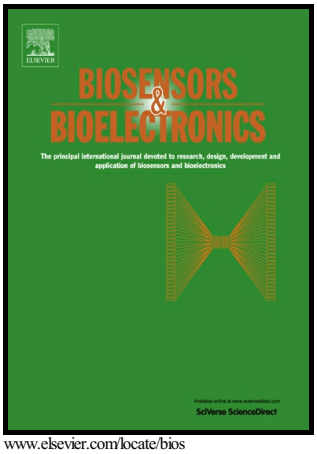

www.elsevier.com/locate/bios

PII: S0956-5663(16)31083-1
DOI: http://dx.doi.org/10.1016/j.bios.2016.10.068
Reference: BIOS9290

To appear in: *Biosensors and Bioelectronic*

Received date: 5 September 2016
Revised date: 20 October 2016
Accepted date: 24 October 2016

Cite this article as: Ya Gao, Xilei Deng, Wei Wen, Xiuhua Zhang and Shengfu Wang, Ultrasensitive paper based nucleic acid detection realized by three dimensional DNA-AuNPs network amplification, *Biosensors and Bioelectronic* http://dx.doi.org/10.1016/j.bios.2016.10.068

Ultrasensitive paper based nucleic acid detection realized by three-dimensional DNA-AuNPs network amplification

Ya Gao[b], Xilei Deng[b], Wei Wen[a,b], Xiuhua Zhang[a,b], Shengfu Wang[a,b*]

[a]Hubei Collaborative Innovation Center for Advanced Organic Chemical Materials, Hubei University, Wuhan 430062, China

[b]Ministry-of-Education Key Laboratory for the Synthesis and Application of Organic Functional Molecules, College of Chemistry and Chemical Engineering, Hubei University, Wuhan 430062, China

[*]Corresponding author: Tel.: +86 27 88663043; fax: +86 27 88663043, wangsf@hubu.edu.cn

Abstract

A novel three-dimensional DNA-AuNPs network structure amplification strategy was employed to design a lateral flow biosensor by introducing streptavidin coated gold nanoparticles (Au-SA) in this paper. They act as amplification probes which aggregate numerous gold nanoparticles (AuNPs) on test line by forming a three-dimensional DNA-AuNPs network structure in the presence of target. Sensitive detection of nucleic acid with point-of-care analysis is significant for infectious agent, early diagnosis and treatment of genetic diseases. The use of these particles in rapid ultrasensitive point of care (POC) lateral flow assays lead to a linear range from 0.1 pM to 250 nM with a limit of detection of 0.01 pM without polymerase chain reaction (PCR). The proposed method could increase the sensitivity by 4 orders of magnitudes than traditional sandwich assays labeled with AuNPs. Furthermore, the assay owns good reproducibility and stability, which will prove practical diagnostic applications.

Keywords: Lateral flow assay, Gold nanoparticles, Nucleic acid, Network amplification

1. Introduction

Lateral flow platforms have become an excellent candidate for the identification of clinically relevant analytes because they are disposable, rapid, portable, user-friendly and cost-effective. In a typical lateral flow assay, reporter particles are transported by capillary action in a porous material and accumulate to form a visible or fluorescent line under the presence of analytes. Presently, there is a growing interest in the development of lateral flow detection of cancer biomarkers (Qin et al., 2015), metal ions (Mazumdar et al., 2010), proteins (Xu et al., 2009, Hwang et al., 2016), viruses (Kim et al., 2015), and nucleic acid (Ciaranello et al., 2011, Fu et al.,2016). Nucleic acid detection is the gold standard for diagnosis of many infectious diseases. For instance, because infants may harbor maternal antibodies against infectious diseases for a period of time after birth, early infant diagnosis requires detection of proviral DNA or viral RNA (Palecek et al., 2001). Most of nucleic acid assay strategies such as Northern, Southern, Western blotting, and polyacrylamide gel electrophoresis require tedious experimental procedures, costly and sophisticated equipments that may not be available in many laboratories. For example, real-time polymerase chain reaction (PCR) requires three different thermal cycling, electrophoresis post processing or fluorescent labeling, which lead to the requirement of highly trained personnel and costly equipments (Chen et al., 2008). As a result, an affordable on-site technique for fast, sensitive, user-friendly nucleic acid detection with high efficiency has become indispensable and urgently needed. Researchers have successfully devised the lateral flow nucleic acid biosensors, which can enable visual detection of DNA fragments without instrumentations (Palecek et al., 2001). The highly sensitive detection of nucleic acid is necessary in clinical diagnosis, genetics therapy, drug discovery, food safety and warning against biowarfare agents. (Drummond et al., 2003, Gooding, J. J., 2002)

Among all kinds of reporter particles, AuNPs are most commonly used in LFA because of their long-terms stability, and good biocompatibility with proteins, DNA, and RNA (Hou et al., 2007). AuNPs possess distinct physical and chemical attributes including high surface-to-volume ratio, excellent biocom-patibility, and unique optoelectronic properties (surface plasmon resonance) and provide a well-suited platform for colorimetric sensing of target analytes (Saha et al., 2012, Howes et al., 2014). Several alternative labels such as fluorescein (Lee et al., 2013), quantum dots (Hu et al., 2016), and carbon nanotubes (Qiu et al., 2015) have been explored in recent years to form novel read-out signal. Fluorescent nanoparticles and quantum dots label have been shown higher sensitivity and wider dynamic range than LFA using conventional AuNPs (Lee et al., 2013). Unfortunately, fluorescent dyes require continuous excitationare because they are prone to photobleaching, which leads to costly and complex readout device. Apart from this, fluorescent nanoparticles are also limited by background autofluorescence at the wavelengths of the reporter's emission (Lee et al., 2013, Freeman et al., 2012, Juntunen et al., 2012). And an easy-distinct red band formed by AuNPs act clearer color contrast than LFA that use CNTs ect. Accordingly, compared with all these alternative labels, AuNPs might be weak in sensitivity, but they are easily recognizable and need no costly and complex readout device. Hence when it comes to practical, AuNPs still occupies the unshakable status. Consequently, an effective amplification strategy for AuNPs labeled lateral flow biosensors is crucially important. Amplification methods reported in the past mainly focus on enzyme catalytic reactions (Mao et al., 2009, Qin et al., 2015). They require specific conditions for enzymatic reactions, e.g., thermal cycles, and special storage for protein enzymes that may be difficult for resource-limited sites (Chen et al., 2015).

In this work, we reported a novel scheme: a three-dimensional network composed of AuNPs and

DNA amplified effect for sensitive and quantitative visual detection of single-stranded DNA. A 30-base nucleotide sequence characteristic of Hepatitis B Virus (targHBV) was selected as a model. A thiolated oligonucleotide (DetProbe) and an oligonucleotide both thiolated and biotinylated (HS-ssDNA-Bio) were used for conjugation with AuNPs. The sensitivity of the biosensor was further enhanced by using AuNPs labled probes (detProbe-Au-ssDNA) and streptavidin coated AuNPs. Amplification method proposed in this work was simple, efficient, easy to operate, time-saving and low requirements, showed great potential in application for point-of-care detection of nucleic acid.

2. Materials and methods

2.1. Chemicals and materials

Trisodium citrate, hydrogen tetrachloroaurate (III) trihydrate ($HAuCl_4 \cdot 3H_2O$), trehalose, sucrose, Tween-20, Tris (2-carboxyethyl) phosphine (TCEP), TritonX-100, deoxyadenosine triphosphate (DATP), sodium tetra borate decahydrate ($Na_2B_4O_7 \cdot 10H_2O$), sodium phorhoate tribasic dodecahydrate ($Na_3PO_4 \cdot 12H_2O$), boric acid (H_3BO_3), phosphotungstic acid hydrate ($H_3O_4PW_{12} \cdot xH_2O$), phosphate buffer saline (pH7.4), human serum, bovine serum albumin (BSA), streptavidin (SA) were purchased from Promega (USA). DT2032 portable strip reader, CTD300P programmable strip cutter, HM3030 dispenser and polyester fiber (VL78, CH27) were purchased from Shanghai KinbioTech. Co., Ltd. Shanghai, China. Nitrocellulose membrane (HFB18002, HFC18002, HFC13502) was purchased from Millipore (Billerica, MA). Transmission electron microscopic (TEM) images were obtained from FEI Tecnai G20 (America). Single-strand DNA were synthesized and purified by Sangon (Shanghai, China), sequences are listed as follows:

DetProbe: 5'-HS-$(CH_2)_6$-AAAAAAAAAATACCACATCATCCAT-3'

T-DNA: 5'-ATAACTGAAAGCCAAAAAAAAAAAA-Biotin-3′

C-DNA: 5'-Biotin-AAAAAAAAAAATGGATGATGTGGTA-3'

HS-ssDNA-Bio: 5'-HS-$(CH_2)_6$-AAACCGTCTCCTTAGACCTTAGGG-Biotin-3'

TargHBV: 5'-TTGGCTTTCAGTTATATGGATGATGTGGTA-3'

All chemicals used in this study were of analytical reagent grade and were purchased from standard commercial sources. Ultra-pure (DI, > 18.25 MΩ) water from a Millipore Milli-Q water purification system (Billerica, MA) was used to prepare all solutions in this work.

2.2 Preparation of streptavidin coated AuNPs

AuNPs with average diameter 15±2.5 nm were prepared following the well-established citrate reduction method (Qin et al., 2016). All glassware was cleaned with freshly prepared aquaregia and rinsed with ultra-pure (DI, > 18.25 MΩ) water. 100 mL of 0.01wt% $HAuCl_4$ aqueous solution was brought to bumping with stirring. Next, 2.7 mL of 1wt% trisodium citrate solution was added. After a few minutes the solution resulted in dark red and kept it boiling for 15 min. Streptavidin-coated AuNPs were prepared according to modifications of literature protocol. (Grabar, et al., 1995, Lim et al., 2012, Chapman et al., 2015). The AuNPs solution was 10-fold concentrated and re-suspended in 20 mM borate buffer (pH=7.4). 400 μL of different concentration (0~100 μg/mL) of streptavidin dissolved in borate buffer was added to 600 μL of AuNPs solution in 50 μL increments, vortexing after each addition. After 1 hour, 300 μL of BSA (20 mg/mL) was added, and the suspension was left overnight at 4℃. The streptavidin-coated AuNPs was purified by centrifugation at 4500 g for 4 times by replacing supernatant with borate buffer. The particle morphology was verified by transmission electron microscopy (FEI Tecnai G20, America) and UV-Vis spectra (UV-2700, Shimadzu Co., Japan). 2.0wt% phosphotungstic acid solution served as the staining agent in transmission electron microscopy.

2.3 Preparation of detProbe-Au-ssDNA conjugates

800 μL of different molar ratios of detProbe and HS-ssDNA-Bio, as well as 400 μL of TCEP (1 mM) were added to 1.2 mL of 10-fold concentrated AuNPs above-mentioned, stirring at room temperature for 1 hour，followed by adding 800 μL of dATP under stirring. After 30 min of the above reaction, the conjugates were kept at 4℃ for 4 h to stabilize the conjugates. The detProbe-Au-ssDNA conjugates obtained were purified with 5% PBSB (5wt% BSA in PBS buffer) by centrifuge at 12 000 rpm for 15 min for each time, and re-diffused in 1.2 mL of aqueous solution containing 10% sucrose, 0.25% Tween-20, 5% BSA, and 20 mM $Na_3PO_4 \cdot 12H_2O$, finally stored at 4℃before further use.

2.4 Assembly of Lateral Flow Strips.

The LFA test strip for HBV nucleic acid detection was composed of a sample pad (Kinbio Tech.Co., Ltd, Shanghai, China), nitrocellulose membrane (Millipore, Bedford, MA, USA), and absorbent pad (Kinbio Tech.Co., Ltd, Shanghai, China). The three parts of strips were fabricated as shown in Figure 1A, wherein the ends of the components overlapped about 2 mm. To ensure a smooth flow of the sample solution from the sample pad to the absorbent pad via capillary action, the sample pad was pretreated by dipping in the sample pad buffer (pH=8.0) containing (0.15 M NaCl, 0.02 M Tris-HCl, and 0.25% TritonX-100) for 1 h, and dried at 37 ℃. Meanwhile, T-DNA and C-DNA were immobilized on NC membrane respectively by conjugated with streptavidin as previously reported (Qin et al., 2015). To be specific, 200 μL of T-DNA (10 μM) were mixed with 20 μL of streptavidin (2 mg/mL), then vortexed and cultivated for 1h. Next remove redundant T-DNA by centrifugation in Millipore's Amicon® Ultra-15 centrifugal filter devices, the same treatment were conducted to C-DNA. The two solutions were finally dispensed onto membrane using a HM3030 dispenser (Kinbio Tech.Co., Ltd, Shanghai, China) to form a test line and a control line, distance between the two adjacent lines was 5 mm. The strip was subsequently dried overnight at 37℃and stored under 4℃for further use.

2.5 Analytical Procedure

Sample solution containing a desired concentration of HBV DNA target in PBS and detProbe-Au-ssDNA conjugates were mixed and cultivated for 15 min. Then Au-SA were sonicated for 120 s and added. The whole mixture was vortexed and cultivated for another 15 min. After applying the obtained solution to sample pad, the strips was washed by 30 μL of 5wt% PBSB. After 10 min, the cassette containing the test strip was inserted into a portable strip reader instrument, a "GoldBio strip reader" software was used to analyze the recording of the optical intensity of the red band on the test line and quantify the analyte. Unamplified lateral flow assay used for comparison was conducted as well. HBV DNA target sample solution and detProbe-Au-ssDNA conjugate were mixed and cultivated for the same time as amplified assay (30 min), then applied the mixture to sample pad. The rest parts of the assay procedure were in accordance with amplified test.

3. Results and discussion

3.1 Design principle of the strip biosensor

We developed amplified lateral flow assay by coupling DNA sandwich detection with AuNPs-DNA network structure. Firstly, AuNPs were prepared followed a citrate reduction method (Qin et al., 2016) for the synthesis of Au-SA and nucleic-acid-functionalized AuNPs. Streptavidin were coated onto the surface of AuNPs via the well-known electrostatic adsorption procedure (Grabar, et al., 1995, Lim et al., 2012). In another respect, two kinds of single-stranded DNA were functionalized to gold surfaces, which included a detection probe (detProbe) partially complementary to target DNA and an auxiliary probe for gathering Au-SA. A schematic of the detection design was shown in Figure 1. The LFA test strip was composed of sample pad, nitrocellulose membrane, and absorbent pad. This test was begun

with the mixture of samples, detProbe-Au-ssDNA conjugates, as well as Au-SA loading onto the sample pad, then migrated by capillary force. Then the complexes were captured by the T-DNA via Watson-Crick base pairing between detProbe and half of targHBV. When target appears, the analyte was sandwiched between the capture DNA probe (immobilized on the test line) and the detection DNA probe which have attached to the surface of AuNPs. Meanwhile, a three-dimensional network composed of AuNPs and DNA was formed and captured on test line, resulting in a visible deep red band. As the liquid continued migrating, the detProbe-Au-ssDNA conjugates and Au-SA were directly trapped by the C-DNA to form a red band on control line. In the absence of targHBV, the complex should flow past the test line without interaction and was only captured by the control line. Figure 1B revealed the reaction on test line and control line in the presence and absence of target respectively. And amplification mechanism was shown in Figure 1C. The result was regarded positive when two red bands appeared on the both test line and control line, and negative when only the control line appeared (Figure 1D). An invalid result was the one with only a test line or no line. Also, the signal on the test line can be quantified by DT2032 portable strip reader.

3.2 Characterization of the Au-SA

The prepared AuNPs were functionalized with streptavidin via the electrostatic adsorption procedure (Grabar, et al., 1995, Lim et al., 2012). Figure 2C and 2D showed transmission electron microscopy images of AuNPs whereas Figure 2A and 2B were images of the Au-SA. It was observed that Au-SA were well dispersed in solution, with the average particle size of 15±2.5 nm and a uniform shell of ~4 nm, which coordinate with the diameter of streptavidin (4 nm). Consequently, we inferred that streptavidin was single-layer coating on the surface of AuNPs.

3.3 Optimization of fabrication and assay parameters

3.3.1 Optimization of streptavidin concentration

To achieve the proper conditions of DNA-AuNPs network amplified LFA, we systematically optimized the experimental parameters. First, in order to verify a suitable streptavidin concentration for covering a full monolayer on the surface of AuNPs, we applied increasing concentrations of streptavidin to AuNPs solution. UV-Vis spectra were used to indicate the adsorption of single and streptavidin coated gold nanoparticles generated by their surface plasmon resonance. Figure 3e showed that λ_{max} of single AuNPs solution appeared at 521 nm. Different shift of λ_{max} emerged when AuNPs were functionalized with different concentrations of SA. As shown in Figure 3a and Figure 3c, an insufficient covering of the protein onto AuNPs resulted in aggregation because of electrostatic absorption. When higher than 60 μg/mL SA was applied to citrate stabilized AuNPs, λ_{max} shifted to a stable peak (525.5 nm), which was 4.5 nm larger than single AuNPs (521 nm).

From another perspective, AuNPs were still covered with citrate molecules that have carboxyl groups which conducted negative charges under a deficiency of SA. Agglomeration of the colloid took place once Na^+ ions were induced. The process was accompanied by a color change of solution. On the contrary, a sufficient quantity of streptavidin molecules was added to ensure that AuNPs were full coated, AuNPs would be highly stable against salt in solution (Li et al., 2009) and no agglomeration and color change would be observed. Therefore, as a supplementary means to judge if AuNPs surface were full covered, 10% NaCl solution was added to Au-SA. As a consequence, 600 μL of AuNPs coated with higher than 60 μg/mL SA were still wine red, with the decrease of concentration of SA, solution turned to be purple. Figure 3 revealed the effect of SA in preventing non-crosslinking aggregation of AuNPs by adding 10% NaCl. Distinct color change could be observed when concentration of SA was relatively low, the outcome was in agreement with the results of UV-Vis spectra.

3.3.2 Optimization of the dosage of Au-SA

An important parameter is the dosage of Au-SA in the assay process. Increasing the volume applied to samples was found to improve the sensitivity of the assay, and the optimum sensitivity was observed at 30 μL Au-SA (Figure S1), but obvious deterioration was observed over 30 μL. The deterioration may caused by space hindrance if too much Au-SA was attached to detProbe-Au-ssDNA conjugates.

3.3.3 Optimization of the ratio of DNA

Thiolated DNA was immobilized on the surface of AuNPs through self-assembling via Au-S bonds. Two thiolated DNA played different roles in this work, and the ratio of them on AuNPs would affect the response of lateral flow assay. Five kinds of molar ratios were tested to reach a maximum efficiency. As shown in Figure S2A, the peak area of test line and the P/N ratio were used to measure amplification performance. The signal increased with decreasing molar ratio from 3/1 to 1/1 and reached a maximum value at 1/1. But with the continued increase of HS-ssDNA-Bio, a relatively sharp signal decline emerged. Also, the variation tendency of P/N ratio was in accordance with that of peak area. There is a competitive effect between two thiolated DNA, presumedly, an excess quantity of HS-ssDNA-Bio onto AuNPs cause reduction of chance of complimentary reaction between detProbe and targHBV which directly decrease signal on test line. So, in order to retain optimized assay conditions with high signal intensity but low background, a molar ratio of 1/1 was chosen in this experiment.

3.3.3 Optimization of sample application strategy

Typically, two different sample application strategies were attempted in our work. Method 1 was to mix detProbe-Au-ssDNA conjugates with targHBV solution, cultivate for 30 min, then Au-SA was

added. Method 2 was to mix all three solutions aforementioned, vortex and then cultivate. Seen from peak area of test line (Figure S2B), we obtained a stronger signal followed method 1. The weaker signal in method 2 may result from a steric hindrance for targHBV to match with detProbe on the surface of AuNPs in the course of competing with Au-SA.

3.3.3 Optimization of NC membrane type

The most important element of a lateral flow strip is nitrocellulose membrane. It was known that flow velocity varied among different NC membrane types because of their different pore sizes, which affect reaction efficiency of the assay and result in difference of sensitivity. To obtain high signal intensity and P/N ratio, three kinds of commercial nitrocellulose membranes (Millipore HFB180, HFC180 and HFC135) were applied to the DNA-AuNPs network amplified lateral flow assay (LFA). As shown in Figure S2C, lateral flow strips that use HFB18002 membrane performed best, and it was chosen for the whole work. It was obvious that the high signal intensity and P/N ratio owed to its smaller pore size.

3.4 Analytical performance

Under optimized assay conditions, the sensitivity of the three-dimensional DNA-AuNPs network amplified lateral flow assay was investigated. Serially diluted targHBV solutions were spiked into buffer solution and human serum samples, then mixed with detProbe-Au-ssDNA and Au-SA in order. And the solution was loaded onto sample pad of the lateral flow strips respectively, finally analyzed by the portable strip reader. As our expectation, only one red band was formed on control line in the absence of targHBV, two red bands were formed on both two lines in the presence of targHBV. In the meantime, the signal intensity of test line increased with the increasing of targHBV concentration. As shown in Figure 4, the test showed a calibration curve exhibiting a good linear relationship between the

peak area of test line and the logarithm of the target concentration within a linear range from 0.1 pM to 250 nM, and a reliable correlation coefficient (R^2=0.99). The LOD (limit of detection) turned out to be 0.01 pM (based on S/N=3). Therefore, it could be applied in detection of nucleic acid qualitatively and quantitatively. And three duplicate measurements at different target concentrations were conducted to gain the error bar. Results were compared between unamplified lateral flow assay and network amplified assay (Figure 4). It was obvious that the fitting curve of unamplified lateral flow assay is steeper in Figure 4. We can infer that the sensitivity of unamplified assay was relatively low. The LOD (limit of detection) of unamplified lateral flow assay turned out to be 0.1 nM with a linear range from 0.5 nM to 100 nM. On the contrary, the proposed method in this paper could increase the sensitivity by 4 orders of magnitudes than traditional sandwich assays and offers a wider linear range. We also compared performances of nucleic acid biosensors with different material and method in table S3. It was obvious that our amplification method promised a relatively low LOD without robust read-out device.

3.5 Selectivity, stability and reproducibility

Recovery studies (Table S1) were conducted to evaluate the precision and reproducibility of the proposed method by executed the intra-assay and inter-assay. We analyzed three standard samples with low (0.02 nM), medium (0.2n M), and high (2 nM) levels of targHBV concentrations. The intra-assay was conducted within one day with five samples of each concentration. Meanwhile the inter-assay was conducted once in each two days for five times of repeat. According to Table S1, the CV value of the intra-assay and inter-assay ranged from 3.38 to 6.24 and 3.72 to 7.28 respectively, which indicated good precision and reproducibility. Hence the further application of the method is of good potential.

Optical response of three kinds of non-complementary DNA in the network amplified LFA were observed. According to the histogram (Figure S3), in the presence of 0 nM targHBV, or 10 nM three noncomplementary DNA respectively, the signals were extremely weak and negligible. And in the mixtures of 0.1 nM targHBV and 10 nM non-complementary DNAs, the response of target has not been affected. The non-specific binding on the test line was comparatively low. We also tested the one-base mismatched DNA on these strips, unfortunately they couldn't differentiate one-mismatched DNA and completely matched DNA (results not shown). In further work we will devote to one-base mismatched DNA detection by introducing the hairpin DNA detection probe.

The stability of the Au-SA and the test strips was evaluated by retesting with increasing storage time with 0.1 nM targHBV. As shown in Figure S4A, Au-SA kept structure and bioactivity after 2 months' storage time under 4℃. On the other hand, the stability of test strips was observed, the signal intensity of test strips after different time length of preservation were close (Figure S4B), indicating the excellent analytical stability of test strips.

3.6 Determination of nucleic acid in human plasma samples

To further demonstrate the reliability and practicability of the developed network amplified LFA, the spiked recovery experiment was conducted. Blank human plasma samples were spiked with different concentrations of targHBV and then measured by the network amplified LFA. As shown in Table S2, with the increasing concentration of targHBV, the mean recoveries of the analyte ranged from 92.70% to 107.84%, which indicate the good accuracy of our proposed network amplified LFA.

4. Conclusions

In summary, size uniformed streptavidin coated AuNPs were successfully prepared with electrostatic adherence. Not only being a label, they also possess a potential magnified effect in the

assay. These nanoparticles are of highly stability, and act as amplification probes aggregating numerous AuNPs on test line by forming a three-dimensional DNA-AuNPs network structure in the presence of target. In our work, the detectable response was dramatically enhanced, the LOD reached 0.01 pM under optimal conditions, which was four orders of magnitude lower than that of unamplified (0.1 nM). The CVs of intra-assay and inter-assay were below 10%. Our proposed method could realize on-site test without complicated process, expensive machine, or highly qualified personnel. A rapid, low cost, and highly sensitive LFA was put forward for nucleic acid detection. It provides promising and versatile opportunities for the analysis of infectious agent and point-of-care diagnosis of genetic diseases. However, in this work we only detected short ssDNA, which limited its potential application, because most natural DNA exists in long double-stranded form. Our next goal is to apply this device into dsDNA detection and long DNA with secondary structures in real samples. What's more, the amplification concept can be extended to visually detection of protein biomarkers as long as the DNA probes were replaced into the relevant aptamers. All these idea will be investigated in our further work.

Acknowledgements

This work was supported by the National Natural Science Foundation of China (No. 21475032).

References

Baryeh, K., Liu, G. D., 2015. Biosens. Bioelectron. 64, 367-372.

Chapman, R., Lin, Y. Y., Burnapp, M., Bentham, A., Hillier, D., Zabron, A., Khan, S., Tyreman, M., Stevens, M. M., 2015. ACS Nano, 9, 2565–2573.

Chen, S., Chu, L. T., Yeung, P. P., Zhao, Z. C., Bao, Y. Y., Chan, M. S., Lo, P. K., Chen, T. H., 2015.

ACS Appl. Mater. Interfaces. 7(41). 22821-22830.

Chen, L., Lee, S., Lee, M., Lim, C., Choo, J., Park, J. Y., Lee, S., Joo, S. W., Lee. K. H., Choi, Y. W. 2008. Biosens. Bioelectron., 23(12), 1878-1882.

Ciaranello, A. L., Park, J.-E., Ramirez-Avila, L., Freedberg, K. A., Walensky, R. P., Leroy, V., 2011. BMC Med. 9, 59-59.

Drummond, T. G., Hill, M. G., Barton, J. K., 2003. Nat. Biotechnol. 21,1192-1199.

Fu, X. L, Cheng Z. Y., Yu, J., Choo, P., Chen, L. X., Choo, J., 2016. Biosens. Bioelectron., 78, 530-537.

Freeman, R., Willner, B., Willner, I., Larmour, I. A., Faulds, K., Graham, D., Han, H., 2012. Functional Nanoparticles for Bioanalysis, Nanomedicine, and Bioelectronic Devices. 1.

Grabar, K.C., Freeman, R.G., Hommer, M.B. Natan, M.J., 1995. Anal. Chem. 67, 735-743.

Gooding, J. J., 2002. Electroanalysis. 14, 1149-1156.

Hou, S. Y., Chen, H. K., Cheng, H. C., Huang, C. Y., 2007. Anal. Chem. 79, 980-985.

Howes, P. D., Rana, S., Stevens, M. M., 2014. Chem. Soc. Rev. 43, 3835-3853.

Hu, J., Zhang, Z. L., Wen, C. Y., Tang, M., Wu, L. L., Liu, C., Zhu, L. and Pang, D. W., 2016. Anal. Chem. 88, 6577-6584.

Hwang, J. K, Lee S. Y., and Choo J. B. , 2016. Nanoscale. 8, 11418-11425.

Juntunen, E., Myyryläinen, T., Salminen, T., Soukka, T., Pettersson, K., 2012. Anal. Biochem. 428, 31-38.

Kim, J. K., Adhikari, M., Dhamane, S., Hagström, A. E. V., Kourentzi, K., Strych, U., Willson, R. C., Conrad, J. C., 2015. ACS Appl. Mater. Interfaces. 7, 2891-2898.

Lee, L. G., Nordman, E. S., Johnson, M. D., Oldham, M. F., 2013. Biosensors. 3, 360-373.,

Li, X., Jiang, L., Zhan, Q., Qian, J., He, S., 2009. Colloid. Surface. A, 332, 172-179.

Lim, S., Koo, O. K., You, Y. S., Lee, Y. E, Kim, M. S., Chang, P. S., Kang, D. H. Yu, J. H., Choi, Y. J. & Gunasekaran S., 2012. Scientific Reports, 2: 456.

Mazumdar, D., Liu, J., Lu, G., Zhou, J., Lu, Y., 2010. Chem. Commun. 46, 1416-1418.

Mao, X., Ma, Y. Q., Zhang, A. G., Zhang, L. R., Zeng, L. W., Liu, G. D., 2009. Anal. Chem. 81, 1660-1668.

Palecek, E.; Fojta, M. 2001. Anal. Chem. 73, 75A-83A.

Qin, C.Y., Wen, W., Zhang, X. h., Gu, H.S., Wang, S. F., 2015. Chem. Commun. 51, 8273-8275.

Qiu, W. W., Xu, H., Takalkar, S., Gurung, A. S., Liu, B., Zheng, Y. F., Guo, Z. B., Baloda, M., Baryeh, K., Liu, G. D. 2015. Biosens. Bioelectron., 64, 367–372.

Qin, C. Y., Wen, W., Zhang, X. H., Gu, H. S., Wang, S. F., 2015. Analyst, 140, 7710.

Qin, C.Y., Wen, W., Zhang, X. h., Gu, H.S., Wang, S. F., 2015. Chem. Commun., 51, 8273-8276,

Qin, C.Y., Gao, Y., Wen, W., Zhang, X. H., Wang, S. F., 2016., Biosens. Bioelectron., 79, 522-530.

Saha, K., Agasti, S. S., Kim, C., Li, X., Rotello, V. M., 2012. Chem. Rev. 112, 2739–2779;

Xu, H., Mao, X., Zeng, Q. X., Wang, S. F., Liu, A. N., Liu, G. D., 2009. Anal. Chem. 81, 669–675

Figure 1. Lateral flow test amplified by Au-SA for nucleic acid detection. (A) Schematic representation of configuration of the test strip. (B) Schematic illustration of the detection of nucleic acid using Au-SA enhanced lateral flow assay. (C) Network structure on test line in the presence of targHBV. (D) Interpretation of positive and negative results.

Figure 2. TEM images of Au-SA (A and B) and Au NPs (C and D).

Figure 3. The effect of amount of streptavidin added on the stability of Au-SA. (a). Photograph of Au-SA synthesized with different concentration of streptavidin (0~100 μg/mL). (b). The color change

of Au-SA synthesized with different concentration of streptavidin after adding 10%NaCl. (c). Schematic representation of adequate (A), inadequate (B) and none (C) SA were used to coat Au NPs. (d). After adding 10% NaCl solutions to A (D), B (E) and C (F). (e). The shift of λmax in UV-Vis spectra when AuNPs were functionalized with different concentrations of SA.

Figure 4. (A)Two kind of strips (network amplified and unamplified) linear response for targHBV detection; Error bars indicate the standard errors of three independent experiments. (B)Photograph of the network amplified detection (right) and unamplified detection (left) for 0.001 nM, 0.01 nM, 0.1 nM, 1 nM, 10 nM, 100 nM in PBS**.**

Highlights

- A novel three-dimensional AuNPs-DNA network structure amplification strategy was employed
- to design a lateral flow biosensor (LFB).
- The network amplificated LFB reached a limit of detection of 0.01pM without PCR (polymerase chain reaction).
- The nucleic acid lateral flow assay is enzyme-free and able to clearly distinguish positive and negative samples by naked eyes.
- The assay owns good reproducibility and stability.
- The strategy can be extended to visually detection of protein biomarkers in the future work.